

# 10

---

## *Volterra's population model*

Consider the Volterra model for the population growth [99] of a species within a closed system governed by a nonlinear integro-differential equation

$$\beta \frac{du(t)}{dt} = u(t) - u^2(t) - u(t) \int_0^t u(x)dx, \quad (10.1)$$

subject to the initial condition

$$u(0) = \alpha, \quad (10.2)$$

where  $u(t)$  is the scaled population of identical individuals,  $t$  denotes the time, and  $\beta = c/(ab)$  is a nondimensional parameter in which  $a > 0$  is the birth rate coefficient,  $b > 0$  is the crowding coefficient, and  $c > 0$  is the toxicity coefficient, respectively. For details the reader is referred to Scudo [99], Small [100], TeBeest [101], and Wazwaz [102].

---

### 10.1 Homotopy analysis solution

#### 10.1.1 Zero-order deformation equation

Let  $\lambda > 0$  denote a so-called time-scale parameter. Under the transformation

$$\tau = \lambda t, \quad w(\tau) = u(t) \quad (10.3)$$

Equation (10.1) becomes

$$(\beta \lambda^2) \frac{dw(\tau)}{d\tau} = \lambda [w(\tau) - w^2(\tau)] - w(\tau) \int_0^\tau w(x)dx, \quad (10.4)$$

subject to the initial condition

$$w(0) = \alpha. \quad (10.5)$$

It was shown by Small [100] that a rise occurs along the solution curve that will reach a peak and then followed by an exponential decay. So, it is reasonable to express  $w(\tau)$  by a set of base functions

$$\{\exp(-n\tau) \mid n \geq 1\} \quad (10.6)$$

in the form

$$w(\tau) = \sum_{n=1}^{+\infty} a_n \exp(-n\tau), \quad (10.7)$$

where  $a_n$  is a coefficient. This provides us with the so-called *rule of solution expression* of  $w(\tau)$ . Under the *rule of solution expression* and using (10.5), it is straightforward to choose the initial guess

$$w_0(\tau) = \alpha \exp(-\tau) + \gamma [\exp(-\tau) - \exp(-2\tau)], \quad (10.8)$$

where  $\gamma$  is an auxiliary parameter to be determined later. Under the *rule of solution expression* denoted by (10.7) and from Equation (10.4), it is straightforward to choose

$$\mathcal{L}f = \frac{df}{d\tau} + f \quad (10.9)$$

as the auxiliary linear operator, which has the property

$$\mathcal{L}[e^{-\tau}] = 0. \quad (10.10)$$

From Equation (10.4), we define the nonlinear integro-differential operator

$$\begin{aligned} \mathcal{N}[\Phi(\tau; q), \Lambda(q)] &= \beta \Lambda^2(q) \frac{\partial \Phi(\tau; q)}{\partial \tau} - \Lambda(q) [\Phi(\tau; q) - \Phi^2(\tau; q)] \\ &+ \Phi(\tau; q) \int_0^\tau \Phi(x; q) dx, \end{aligned} \quad (10.11)$$

where  $q \in [0, 1]$  is an embedding parameter,  $\Phi(\tau; q)$  is a function of  $\tau$  and  $q$ , and  $\lambda(q)$  is a function dependent of  $q$ . Let  $\hbar \neq 0$  denote a nonzero auxiliary parameter and  $H(\tau)$  a nonzero auxiliary function, respectively. We construct the zero-order deformation equation

$$(1 - q) \mathcal{L}[\Phi(\tau; q) - w_0(\tau)] = q \hbar H(\tau) \mathcal{N}[\Phi(\tau; q), \Lambda(q)], \quad (10.12)$$

subject to the initial condition

$$\Phi(0; q) = \alpha, \quad (10.13)$$

where  $q \in [0, 1]$  is an embedding parameter.

When  $q = 0$ , it is straightforward that

$$\Phi(\tau; 0) = w_0(\tau). \quad (10.14)$$

When  $q = 1$ , since  $\hbar \neq 0$  and  $H(\tau) \neq 0$ , the zero-order deformation equations (10.12) and (10.13) are equivalent to Equations (10.4) and (10.5), respectively, provided

$$\Phi(\tau; 1) = w(\tau), \quad \Lambda(1) = \lambda. \quad (10.15)$$

Thus, as  $q$  increases from 0 to 1,  $\Phi(\tau; q)$  varies from the initial guess  $w_0(\tau)$  to the solution  $w(\tau)$  of Equations (10.4) and (10.5), so does  $\Lambda(q)$  from the initial guess

$$\Lambda(0) = \lambda_0 \tag{10.16}$$

to the exact time-scale parameter  $\lambda$ . Note that the zero-order deformation equation (10.12) contains the auxiliary parameter  $\hbar$  and the auxiliary function  $H(\tau)$ . The initial guess  $w_0(\tau)$  contains the auxiliary parameter  $\gamma$ . Assume that all of them are properly chosen so that in the whole region  $q \in [0, 1]$  there exist the solutions  $\Phi(\tau; q)$ ,  $\Lambda(q)$  of the zero-order deformation equations (10.12) and (10.13), and also the terms

$$w_n(\tau) = \frac{1}{n!} \left. \frac{\partial^n \Phi(\tau; q)}{\partial q^n} \right|_{q=0}, \tag{10.17}$$

$$\lambda_n = \frac{1}{n!} \left. \frac{\partial^n \Lambda(q)}{\partial q^n} \right|_{q=0}. \tag{10.18}$$

Then, by Taylor's theorem and using (10.14) and (10.16), we expand  $\Phi(\tau; q)$  and  $\Lambda(q)$  in the series

$$\Phi(\tau; q) = w_0(\tau) + \sum_{n=1}^{+\infty} w_n(\tau) q^n, \tag{10.19}$$

$$\Lambda(q) = \lambda_0 + \sum_{n=1}^{+\infty} \lambda_n q^n. \tag{10.20}$$

Assuming that the auxiliary parameters  $\hbar, \gamma$ , and the auxiliary function  $H(\tau)$  are properly chosen so that the above series converge at  $q = 1$ , we have, using (10.15), the solution series

$$w(\tau) = w_0(\tau) + \sum_{n=1}^{+\infty} w_n(\tau), \tag{10.21}$$

$$\lambda = \lambda_0 + \sum_{n=1}^{+\infty} \lambda_n. \tag{10.22}$$

At the  $M$ th order of approximation, we gain

$$w(\tau) \approx w_0(\tau) + \sum_{n=1}^M w_n(\tau), \tag{10.23}$$

$$\lambda \approx \lambda_0 + \sum_{n=1}^M \lambda_n. \tag{10.24}$$

### 10.1.2 High-order deformation equation

For brevity, define the vector

$$\vec{w}_n = \{w_0(\tau), w_1(\tau), \dots, w_n(\tau)\}, \quad \vec{\lambda}_n = \{\lambda_0, \lambda_1, \dots, \lambda_n\}.$$

Differentiating the zero-order deformation equations (10.12) and (10.13)  $n$  times with respect to the embedding parameter  $q$  and then dividing by  $n!$  and finally setting  $q = 0$ , we have the high-order deformation equation

$$\mathcal{L} [w_n(\tau) - \chi_n w_{n-1}(\tau)] = \hbar H(\tau) R_n(\vec{w}_{n-1}, \vec{\lambda}_{n-1}), \quad (10.25)$$

subject to the initial condition

$$w_n(0) = 0, \quad (10.26)$$

where  $\chi_n$  is defined by (2.42) and

$$\begin{aligned} & R_n(\vec{w}_{n-1}, \vec{\lambda}_{n-1}) \\ &= \frac{1}{(n-1)!} \left. \frac{\partial^{n-1} \mathcal{N} [\Phi(\tau; q), \Lambda(q)]}{\partial q^{n-1}} \right|_{q=0} \\ &= \beta \sum_{j=0}^{n-1} w'_{n-1-j}(\tau) \sum_{i=0}^j \lambda_i \lambda_{j-i} - \sum_{j=0}^{n-1} \lambda_j w_{n-1-j}(\tau) \\ &+ \sum_{j=0}^{n-1} \lambda_{n-1-j} \sum_{i=0}^j w_i(\tau) w_{j-i}(\tau) \\ &+ \sum_{j=0}^{n-1} w_{n-1-j}(\tau) \int_0^\tau w_j(x) dx. \end{aligned} \quad (10.27)$$

There are two unknowns:  $\lambda_{n-1}$  and  $w_n(\tau)$ . However, we have only one differential equation (10.25) for  $w_n(\tau)$ . Thus, the problem is not closed and an additional algebraic equation is needed to determine  $\lambda_{n-1}$ . Using (10.8) and (10.27), it is straightforward to get

$$R_1(\vec{w}_0, \vec{\lambda}_0) = \sum_{m=1}^4 a_{1,m} \exp(-m \tau) \quad (10.28)$$

where

$$a_{1,1} = (\alpha + \gamma) \left( \alpha + \frac{\gamma}{2} - \lambda_0 - \beta \lambda_0^2 \right)$$

and  $a_{1,j}$  ( $j = 2, 3, 4$ ) are coefficients. Note that the auxiliary function  $H(\tau)$  is unknown right now. According to the *rule of solution expression* denoted by (10.7) and from Equation (10.25), the auxiliary function should be in the form

$$H(\tau) = \exp(\kappa \tau),$$

where  $\kappa$  is an integer. It is found that, when  $\kappa \geq 1$ , the solution  $w_n(\tau)$  of Equation (10.25) contains a constant term that does not vanish at infinity. This disobeys the *rule of solution expression* denoted by (10.7). When  $k \leq -2$ , the solution  $w_n(\tau)$  of Equation (10.25) does not contain the term  $\exp(-2\tau)$ , and this disobeys the so-called *rule of coefficient ergodicity*. So,  $\kappa$  should be either 0 or 1. When  $\kappa = 1$ , we cannot give an additional algebraic equation for  $\lambda_0$  so that the problem is still not closed, and this disobeys the *rule of solution existence*. So, only  $\kappa = 0$  is possible, which uniquely determines the auxiliary function

$$H(\tau) = 1. \tag{10.29}$$

In this case, the right-hand side of the first-order deformation equation (10.25) contains the term  $\exp(-\tau)$ . Then, according to (10.10),  $w_1(\tau)$  contains the term  $\tau \exp(-\tau)$ , which disobeys the *rule of solution expression* denoted by (10.7). To obey the *rule of solution expression*, we had to enforce  $a_{1,1} = 0$ , i.e.,

$$(\alpha + \gamma) \left( \alpha + \frac{\gamma}{2} - \lambda_0 - \beta \lambda_0^2 \right) = 0, \tag{10.30}$$

which provides us with the additional equation for  $\lambda_0$  with the positive solution

$$\lambda_0 = \frac{\sqrt{1 + 2\beta(\gamma + 2\alpha)} - 1}{2\beta}. \tag{10.31}$$

Thereafter, it is straightforward to get the solution

$$w_1(\tau) = \hbar \sum_{m=2}^4 \left( \frac{a_{1,m}}{m-1} \right) (\exp^{-\tau} - \exp^{-m\tau}). \tag{10.32}$$

In general, the term  $R_n(\vec{w}_{n-1}, \vec{\lambda}_{n-1})$  can be generally expressed by

$$R_n(\vec{w}_{n-1}, \vec{\lambda}_{n-1}) = \sum_{m=1}^{2(n+1)} a_{n,m} \exp(-m \tau), \tag{10.33}$$

where  $a_{n,m}$  is a coefficient, and we can get  $\lambda_{n-1}$  by enforcing

$$a_{n,1} = 0. \tag{10.34}$$

In this way, we successively gain the solution

$$w_n(\tau) = \chi_{n-1} w_{n-1}(\tau) + \hbar \sum_{m=2}^{2(n+1)} \left( \frac{a_{n,m}}{m-1} \right) (e^{-\tau} - e^{-m\tau}) \tag{10.35}$$

of high-order deformation equations (10.25) and (10.26).

### 10.1.3 Recursive expression

Considering the importance of Volterra's population model, it is helpful to give an explicit analytic expression of the solution. It is found that  $w_n(\tau)$  can be expressed by

$$w_n(\tau) = \sum_{m=1}^{2(n+1)} b_{n,m} \exp(-m \tau), \quad (10.36)$$

where  $b_{n,m}$  is a coefficient. Substituting it into Equations (10.25) and (10.26), we have the recursive formulae ( $n \geq 2, i \geq 2$ )

$$\lambda_{n-1} = \frac{\Delta_{n,1} - \sum_{j=0}^{n-2} (\lambda_j + \beta\delta_j) b_{n-1-j,1} - \beta b_{0,1} \sum_{i=1}^{n-2} \lambda_i \lambda_{n-1-i}}{(1 + 2\beta\lambda_0)b_{0,1}}, \quad (10.37)$$

$$b_{n,i} = \chi_n \chi_{2n+2-i} b_{n-1,i} + \frac{\hbar (\Pi_{n,i} + \Delta_{n,i} - \chi_{2n+2-i} \Gamma_{n,i})}{(1-i)}, \quad (10.38)$$

$$b_{n,1} = - \sum_{i=2}^{2(n+1)} b_{n,i}, \quad (10.39)$$

where

$$\begin{aligned} \Pi_{n,i} &= \sum_{j=\max\{0, [(i+1)/2]-2\}}^{n-1} \lambda_{n-1-j} d_{j,i}, & 2 \leq i \leq 2(n+1), \\ \Delta_{n,i} &= \sum_{j=0}^{n-1} \sum_{s=\max\{1, i-2(j+1)\}}^{\min\{2(n-j), i\}} b_{n-1-j,s} c_{j,i-s}, & 1 \leq i \leq 2(n+1), \\ \Gamma_{n,i} &= \sum_{j=0}^{\min\{n-1, n-[(i+1)/2\}} (i\beta\delta_j + \lambda_j) b_{n-1-j,i}, & 1 \leq i \leq 2n, \end{aligned}$$

under the definitions

$$d_{n,m} = \sum_{i=0}^n \sum_{j=\max\{1, m-2(n-i+1)\}}^{\min\{2(i+1), m-1\}} b_{i,j} b_{n-i, m-j}, \quad 2 \leq m \leq 2(n+1)$$

and

$$\begin{aligned} c_{n,m} &= -\frac{b_{n,m}}{m}, & 1 \leq m \leq 2(n+1), \\ c_{n,0} &= \sum_{m=1}^{2(n+1)} \frac{b_{n,m}}{m}, \\ \delta_n &= \sum_{i=0}^n \lambda_i \lambda_{n-i} \end{aligned}$$

in which the term  $[x]$  denotes the integer part of  $x$ . From (10.8) we have the first two coefficients

$$b_{0,1} = \alpha + \gamma, \quad b_{0,2} = -\gamma. \quad (10.40)$$

From these two coefficients and using the above recursive formulae, we can successively calculate all coefficients  $b_{n,j}$ . The  $M$ th-order approximation of  $u(t)$  is given by

$$u(t) \approx \sum_{n=0}^M \sum_{m=1}^{2(n+1)} b_{n,m} \exp(-m \lambda t), \quad (10.41)$$

where

$$\lambda \approx \sum_{n=0}^{M-1} \lambda_n. \quad (10.42)$$

When  $M \rightarrow +\infty$  we gain the explicit analytic solution

$$u(t) = \sum_{n=0}^{+\infty} \sum_{m=1}^{2(n+1)} b_{n,m} \exp(-m \lambda t), \quad (10.43)$$

where

$$\lambda = \sum_{n=0}^{+\infty} \lambda_n. \quad (10.44)$$

#### 10.1.4 Convergence theorem

##### **THEOREM 10.1**

*If the solution series (10.21) and (10.22) converge, where  $w_n(\tau)$  is governed by Equations (10.25) and (10.26) under the definitions (10.27) and (2.42), they must be the solution of Equations (10.4) and (10.5).*

Proof: If the solution series (10.21) and (10.22) converge, it is necessary that

$$\lim_{m \rightarrow +\infty} w_m(\tau) = 0. \quad (10.45)$$

Then, using (10.9), (10.25), and (2.42), it holds

$$\begin{aligned} & \hbar H(\tau) \sum_{n=1}^{+\infty} R_n(\vec{w}_{n-1}, \vec{\lambda}_{n-1}) \\ &= \lim_{m \rightarrow +\infty} \mathcal{L}[w_m(\tau)] = \mathcal{L} \left[ \lim_{m \rightarrow +\infty} w_m(\tau) \right] = 0, \end{aligned} \quad (10.46)$$

which gives, since  $\hbar \neq 0$  and  $H(\tau) = 1$ ,

$$\sum_{n=1}^{+\infty} R_n(\vec{w}_{n-1}, \vec{\lambda}_{n-1}) = 0. \quad (10.47)$$

Substituting (10.27) into the above expression and simplifying it, we have

$$\begin{aligned}
 & \beta \left( \sum_{n=0}^{+\infty} \lambda_n \right)^2 \frac{d}{d\tau} \left[ \sum_{n=0}^{+\infty} w_n(\tau) \right] \\
 &= \left( \sum_{n=0}^{+\infty} \lambda_n \right) \left\{ \left[ \sum_{n=0}^{+\infty} w_n(\tau) \right] - \left[ \sum_{n=0}^{+\infty} w_n(\tau) \right]^2 \right\} \\
 &- \left[ \sum_{n=0}^{+\infty} w_n(\tau) \right] \int_0^\tau \left[ \sum_{n=0}^{+\infty} w_n(x) \right] dx. \tag{10.48}
 \end{aligned}$$

From (10.8) and (10.26), we have

$$\sum_{n=0}^{+\infty} w_n(0) = \alpha. \tag{10.49}$$

Comparing these two expressions with Equations (10.4) and (10.5), the solution series (10.21) and (10.22) must be the solution of the Volterra's population model, as long as they are convergent. This ends the proof.

## 10.2 Result analysis

According to Theorem 10.1 we should only focus on ensuring that the solution series (10.21) and (10.22) converge. Note that there exists the integral term

$$\int_0^t u(x) dx$$

in Equation (10.1) and the value

$$\mu = \int_0^{+\infty} u(x) dx \tag{10.50}$$

denotes the total scaled population and thus has an important meaning. Under the transformation (10.3), the above expression becomes

$$\lambda \mu = \int_0^{+\infty} w(\xi) d\xi. \tag{10.51}$$

### 10.2.1 Choosing a plain initial approximation

For the given  $\alpha$  and  $\beta$ , we have freedom to choose the auxiliary parameters  $\hbar$  and  $\gamma$ , which influence the convergence region and rate of the solution series



(10.21) and (10.22). Generally speaking, for any chosen value of  $\gamma$ , we can investigate the influence of  $\hbar$  by plotting the so-called  $\hbar$ -curves (see page 26 and §3.5.1) of  $\int_0^{+\infty} u(x)dx$ . For example, consider the case  $\alpha = 1/10$  and  $\beta = 1/5$ . The corresponding  $\hbar$ -curves of  $\int_0^{+\infty} u(x)dx$  at the 10th order of approximation when  $\gamma = 1, 2, 3, 4$  are as shown in Figure 10.1. Note that the corresponding valid region of  $\hbar$  increases when  $\gamma$  decreases from 4 to 2, but there is no such valid region when  $\gamma = 1$ . From these  $\hbar$ -curves, it is clear that when  $\alpha = 1/10$  and  $\beta = 1/5$ , the approximation series of  $\int_0^{+\infty} u(x)dx$  converges if  $2 \leq \gamma \leq 4$  and  $\hbar$  is chosen in the corresponding valid region. For instance, when  $\gamma = 3$  corresponding to

$$\lambda_0 = 1.27492$$

given by (10.31), the approximation series of  $\int_0^{+\infty} u(x)dx$  is convergent by means of  $\hbar = -1/2$ , as shown in Table 10.1. It is found that, in general, as long as the series of  $\int_0^{+\infty} u(x)dx$  converges, the corresponding series (10.22) of  $\lambda$  also converges, as shown in Table 10.1 for the special case. The homotopy-Padé technique (see page 38 and §3.5.2) greatly enhances the convergence rate of the series of  $\lambda$  and  $\int_0^{+\infty} u(x)dx$ , as shown in Table 10.2. It is found that the  $[m, m]$  homotopy-Padé approximants are independent of  $\hbar$ . Also, as long as the series of  $\int_0^{+\infty} u(x)dx$  converges, the corresponding series (10.21) converges in the whole region  $0 \leq t < +\infty$  to the numerical results [100, 101, 102], as shown in Figure 10.2 for the special case of  $\alpha = 1/10$  and  $\beta = 1/5$ . In this way we can gain the analytic solutions for any given values of  $\alpha$  and  $\beta$ .

## 10.2.2 Choosing the best initial approximation

Note that the initial approximation  $w_0(\tau)$  is determined by the auxiliary parameter  $\gamma$ . Clearly, a better choice of  $\gamma$  should give a better series which approximates the solution more efficiently. At the zero order of approximation we have

$$\lambda \mu \approx \int_0^{+\infty} w_0(x)dx. \quad (10.52)$$

At the first order of approximation it holds

$$\lambda \mu \approx \int_0^{+\infty} w_0(x)dx + \int_0^{+\infty} w_1(x)dx. \quad (10.53)$$

Obviously, we can choose  $\gamma$  in such a way that the zero-order approximation (10.52) is so accurate that its first-order approximation (10.53) cannot give a better result of  $\lambda \mu$ , i.e.,

$$\int_0^{+\infty} w_1(x)dx = 0. \quad (10.54)$$

This gives an algebraic equation

$$24\beta \gamma \lambda_0^2 + 2(6\alpha^2 + 6\gamma + 4\alpha \gamma + \gamma^2)\lambda_0 - 3(4\alpha^2 + 8\alpha\gamma + 3\gamma^2) = 0. \quad (10.55)$$

Solving the set of two algebraic equations (10.30) and (10.55), we can obtain the “best” positive values of  $\lambda_0$  and  $\gamma$  for any given values of  $\alpha$  and  $\beta$ . For example, when  $\alpha = 1/10$  and  $\beta = 1/5$ , the best values of  $\lambda_0$  and  $\gamma$  are

$$\lambda_0 = 1.02682, \quad \gamma = 2.27538. \quad (10.56)$$

The above “best” value of  $\gamma$  explains why the valid region of  $h$  corresponding to  $\gamma = 2$  is longer than that of  $\gamma = 3$  and  $\gamma = 4$ , as shown in [Figure 10.1](#). The corresponding solution series are indeed convergent more quickly, as shown in [Table 10.3](#). Also, the homotopy-Padé technique can greatly accelerate the convergence of the solution series, as shown in [Table 10.4](#). It is interesting that, when  $\alpha = 1/10$  and  $\beta = 1/5$ , the series of the time-scale parameter  $\lambda$  converge to the same value 0.986, although two different values of  $\lambda_0$  are used, as shown in [Tables 10.1 to 10.4](#). Like  $\int_0^{+\infty} u(x)dx$ , the time-scale parameter  $\lambda$  depends upon  $\alpha$  and  $\beta$ . It decreases as the term  $\int_0^{+\infty} u(x)dx$  increases, thus, the time-scale parameter  $\lambda$  might have some physical meanings.

Using the “best” values of  $\gamma$  and  $\lambda_0$  given by (10.30) and (10.55), we can analytically solve Volterra’s population model more efficiently. The convergent analytic results of  $u(t)$  when  $\alpha = 1/10$  and  $\beta = 1/10, 1/5, 1/2, 1$  and  $10$  are as shown in [Figure 10.3](#). The total scaled population  $\int_0^{+\infty} u(x)dx$ , the time-scale parameter  $\lambda$ , and the corresponding best values of  $\gamma$  and  $\lambda_0$  for some  $\alpha$  and  $\beta$  are listed in [Table 10.5](#).

This example illustrates that the homotopy analysis method is valid for nonlinear integro-differential equations.

**TABLE 10.1**

The analytic approximations of  $\int_0^\infty u(x)dx$  and  $\lambda$  given by (10.23) and (10.24) when  $\alpha = 1/10, \beta = 1/5$  by means of  $\gamma = 3, \lambda_0 = 1.27492$ , and  $\hbar = -1/2$ .

Order of approximation	$\int_0^{+\infty} u(x)dx$	$\lambda$
10	1.194	1.014
20	1.196	0.988
30	1.196	0.983
40	1.197	0.983
50	1.197	0.983
60	1.197	0.984
70	1.197	0.985
80	1.197	0.985

**TABLE 10.2**

The  $[m, m]$  homotopy-Padé approximations of  $\int_0^\infty u(x)dx$  and  $\lambda$  when  $\alpha = 1/10, \beta = 1/5$  by means of  $\gamma = 3$  and  $\lambda_0 = 1.27492$ .

$[m, m]$	$\int_0^{+\infty} u(x)dx$	$\lambda$
[5, 5]	1.196	0.982
[10, 10]	1.197	0.987
[15, 15]	1.197	0.986
[20, 20]	1.197	0.986
[25, 25]	1.197	0.986
[30, 30]	1.197	0.986
[35, 35]	1.197	0.986
[40, 40]	1.197	0.986

**TABLE 10.3**

The analytic approximations of  $\int_0^\infty u(x)dx$  and  $\lambda$  when  $\alpha = 1/10, \beta = 1/5$  by means of  $\gamma = 2.27538, \lambda_0 = 1.02682$ , and  $h = -1$ .

Order of approximation	$\int_0^{+\infty} u(x)dx$	$\lambda$
10	1.195	0.997
20	1.197	0.985
30	1.197	0.985
40	1.197	0.986
50	1.197	0.986
60	1.197	0.986
70	1.197	0.986
80	1.197	0.986

**TABLE 10.4**

The  $[m, m]$  homotopy-Padé approximations of  $\int_0^\infty u(x)dx$  and  $\lambda$  when  $\alpha = 1/10, \beta = 1/5$  by means of  $\gamma = 2.27538$  and  $\lambda_0 = 1.02682$ .

$[m, m]$	$\int_0^{+\infty} u(x)dx$	$\lambda$
[5, 5]	1.197	0.986
[10, 10]	1.197	0.986
[15, 15]	1.197	0.986
[20, 20]	1.197	0.986
[25, 25]	1.197	0.986
[30, 30]	1.197	0.986
[35, 35]	1.197	0.986
[40, 40]	1.197	0.986

**TABLE 10.5**

The convergent analytic results and the corresponding “best” values of  $\gamma$  and  $\lambda_0$  for  $\alpha = 1/10$  and different values of  $\beta$ .

$\beta$	$\lambda_0$	$\gamma$	$\int_0^{+\infty} u(x)dx$	$\lambda$
1/10	1.19933	2.48633	1.100	1.000
1/5	1.02682	2.27538	1.197	0.986
1/2	0.75414	1.87701	1.418	0.836
1	0.55274	1.51653	1.627	0.626
10	0.15621	0.57101	2.572	0.157

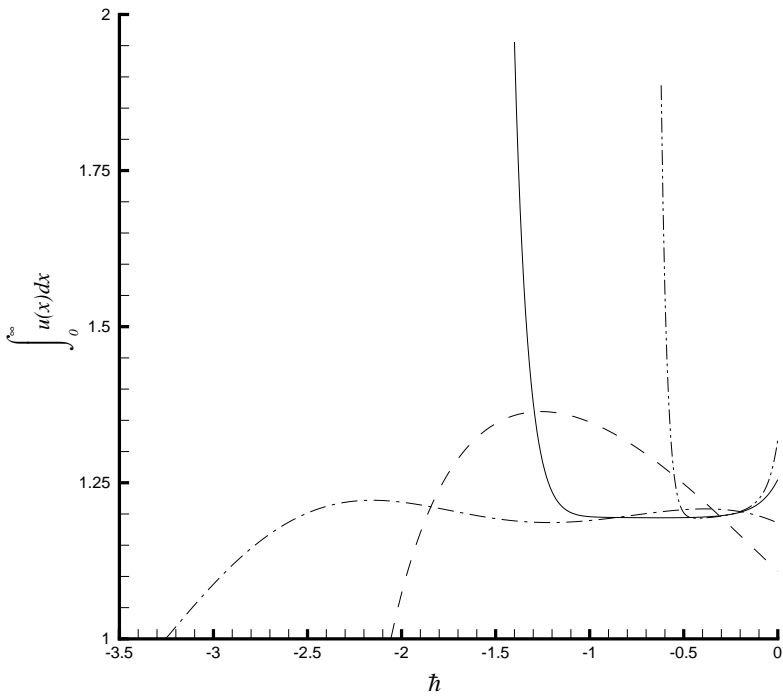


**FIGURE 10.1**

The  $h$ -curves of  $\int_0^{+\infty} u(x) dx$  at the 10th order of approximation when  $\alpha = 1/10$  and  $\beta = 1/5$  with different values of  $\gamma$ . Dashed line:  $\gamma = 1$ ; dash-dotted line:  $\gamma = 2$ ; solid line:  $\gamma = 3$ ; dash-dot-dotted line:  $\gamma = 4$ .

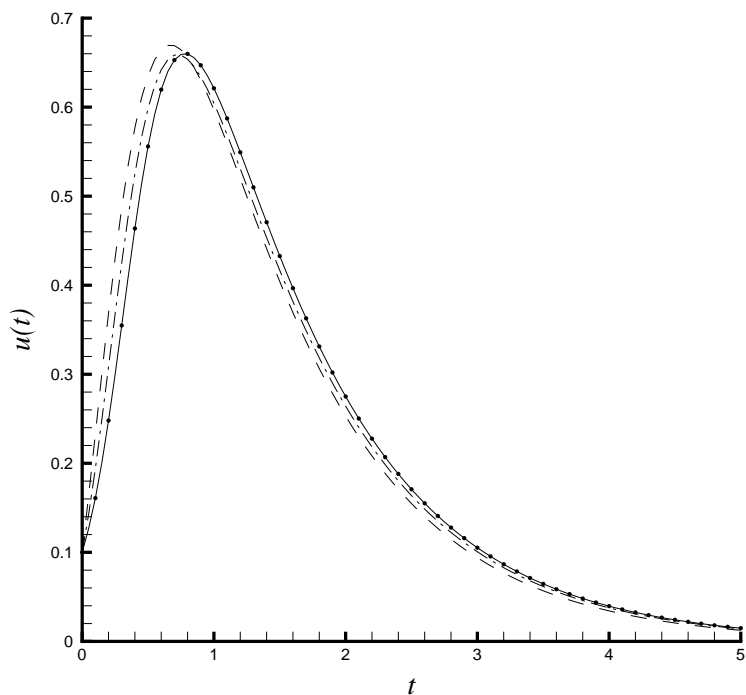


**FIGURE 10.2**

Comparison of the numerical result [100, 101, 102] with the analytic approximations of  $u(t)$  when  $\alpha = 1/10$  and  $\beta = 1/5$  by means of  $\gamma = 3$  and  $\hbar = -1/2$ . Symbol: numerical result; dashed line: 10th-order analytic approximation; dash-dotted line: 20th-order analytic approximation; solid line: 50th-order analytic approximation.

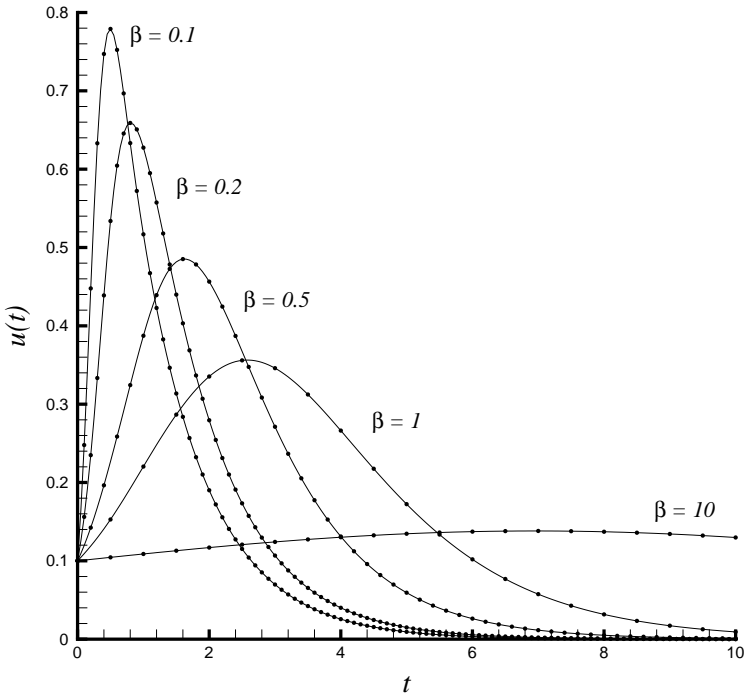


**FIGURE 10.3**

Comparison of the numerical results [100, 101, 102] with the analytic approximations of  $u(t)$  when  $\alpha = 1/10$  and  $\beta = 1/10, 1/5, 1/2, 1, 10$  by means of  $\hbar = -1$  and the “best” values of  $\lambda_0$  and  $\gamma$  given by (10.30) and (10.55). Symbol: numerical result; solid line: analytic results at the 20th ( $\beta = 1/10$ ), 30th ( $\beta = 1/5$ ), 40th ( $\beta = 1/2$ ), 50th ( $\beta = 1$ ), and 50th order ( $\beta = 10$ ) of approximation, respectively.